Available online at www.sciencedirect.com
SCIENCE DIRECT
Polymer 46 (2005) 3758–3766
polymer
www.elsevier.com/locate/polymer

Study of the morphologies and dielectric constants of nanoporous materials derived from benzoxazine-terminated poly(ε-caprolactone)/polybenzoxazine co-polymers

Yi-Che Su[a,b], Wan-Chun Chen[a], Kai-lin Ou[a], Feng-Chih Chang[a,*]

[a]*Institute of Applied Chemistry, National Chiao-Tung University, Hsin-Chu, Taiwan, ROC*
[b]*Union Chemical Laboratories, Industrial Technology Research Institute, Hsin-Chu, Taiwan, ROC*

Received 12 October 2004; received in revised form 4 March 2005; accepted 14 March 2005
Available online 11 April 2005

Abstract

We have generated porous polybenzoxazine (PBZZ) materials by using a B-a type PBZZ as the matrix and various molecular weights of poly(ε-caprolactone) (pa-PCL) as the labile constituent. The slight degree of hydrogen bonding that exists between the two polymers results in micro-phase separation without an excess degree of aggregation occurring. The porous structures form after hydrolysis of the PCL domains; we characterized them using a variety of techniques, including FT-IR spectroscopy, DSC, TGA, FE-SEM, and DEA. At 298 K and 10^5 Hz, we obtained a thin, transparent, and nanoporous film that has a very low dielectric constant (1.95).

Keywords: Polybenzoxazine; Nanoporous; Low dielectric constant

1. Introduction

As feature sizes in microelectronic devices are driven to sub-100-nm dimensions, device performance will no longer be on the scale it has been in the past because of a substantial increase in interconnect delays (RC delay) [1–4] caused by the increased line resistance, capacitive coupling, and cross talk that occurs between smaller and more closely spaced metal lines. Fluorinating polymers and forming porous structures are two major directions that have been followed in the course of developing materials that have low dielectric constants (low k) [1,2,5–7]. Recently, there has been a demand for low-dielectric-constant materials that can decrease the RC delay, power consumption, and cross-talk noise; this demand has stimulated intense efforts in the exploration and applicability of porous materials, especially nanoporous materials [8–11].

Nanoporous and mesoporous materials have potential or are used in many devices, which include sensors, photonic crystals, waveguides, and dielectrics [12,13]. It is becoming increasingly more important to be able to control the pore structures and understand their properties on nano- and micrometer length scales. It is well known that reducing the dielectric constant can be achieved simply by replacing the polymer with air [14,15], which has a dielectric constant of one. Therefore, increasing the pore density will lead to lower-dielectric-constant materials. The size of the voids, however, must be substantially smaller than both the film thickness and any microelectronic features for the gain in the dielectric constant to be realized [1,2]. Suitable porous structures can be prepared from co-polymers comprising a thermally stable or solvent-stable material and a thermally labile or solvent-labile material [12,16,17]; the latter system constitutes a dispersed phase. The greatest challenge in the future will be to reduce the pore size at an even distribution while maintaining the strength within a range acceptable for mechanical and electronic applications.

In this study, we prepared a porous material having a low value for its dielectric constant by treating poly(ε-caprolactone) (PCL) with B-a type polybenzoxazine (PBZZ), which act as the labile and stable constituents, respectively. PCL is a highly crystalline polymer that becomes miscible with several amorphous polymers through the formation of hydrogen bonds [18–20]. A variety of catalysts have been

* Corresponding author. Tel.: +886 3 5727077; fax: +886 3 5719507.
E-mail address: changfc@cc.nctu.edu.tw (F.-C. Chang).

0032-3861/$ - see front matter © 2005 Elsevier Ltd. All rights reserved.
doi:10.1016/j.polymer.2005.03.035

investigated for the ring-opening polymerization (ROP) of ε-caprolactone (ε-CL) to PCL. Co-polymers of PCL are useful because of their biodegradability and polymer blend compatibility. The miscibility of PCL blends or co-polymers depends on self- and inter-association that arises through hydrogen bonding with donor polymers. In addition, PBZZ contains a high density of hydroxyl groups [21–24] that interact with the carbonyl groups of PCL through hydrogen bonding. To prepare a microporous material, it is essential to prepare a well-dispersed microphase-separated labile constituent within a stable matrix. Hence, we modified the PCL's end group to decrease the degree of phase separation.

As shown in Scheme 1, pa-PCL forms covalent bonds with the PBZZ backbone because these pa-PCL compounds possess similar benzoxazine structures. We generated a porous structure by preparing a co-polymer between the matrix phase (PBZZ) and a minor phase that consisted of a solvent (basic)-labile polymer (PCL). We synthesized co-polymers of pa-PCL and PBZZ having different molecular weights. Films of the co-polymers were cast and then heated to effect annealing, which resulted in the nanoscale microphase separation of these two dissimilar blocks. We removed the labile constituent selectively through hydrolysis using $NaHCO_3$, which created pores having the shape of the original co-polymer's morphology. Using this approach, we obtained a porous material having a low dielectric constant.

2. Experimental

2.1. Materials

4-Hydroxybenzyl alcohol, ε-caprolactone and tin(II) 2-ethylhexanoate were purchased from the Acros Chemical Co., USA. Formaldehyde and aniline were purchased from the Aldrich Chemical Co., USA.

2.2. Synthesis of (3-phenyl-3,4-dihydro-2H-1,3-benzoxazin-6-yl)methanol (pa-OH)

The benzoxazine was prepared according to Scheme 1. Thirty seven percent aqueous formaldehyde solution

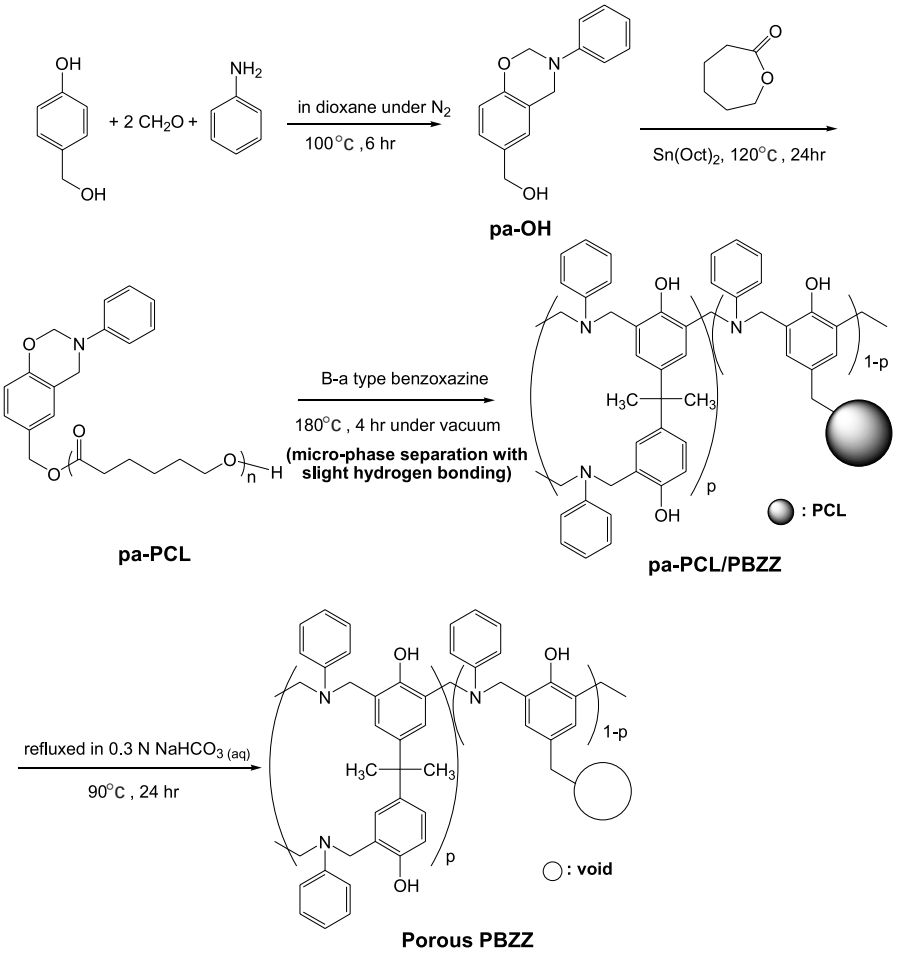

Scheme 1. Syntheses of pa-OH, pa-PCL, pa-PCL/PBZZ and schematic representation of the generation of nanoporous PBZZ films from phase-separated co-polymers.

(6.53 g, 0.08 mol) and dioxane (10 mL) were mixed for 10 min under nitrogen in a three-necked flask placed in an ice bath. Then, the aniline (3.75 g, 0.04 mol) dissolved in dioxane (10 mL) was added slowly using a dropping funnel. The mixture was stirred magnetically for 10 min before 4-hydroxybenzyl alcohol (5 g, 0.04 mol) in dioxane (10 mL) was added. The reaction temperature was raised to 100 °C and the mixture was heated under reflux for 6 h. The solvent was then evaporated under reduced pressure to yield a light-yellow powder. This crude product was dissolved in ethyl ether and washed sequentially with 1 N NaOH and water for three times; the organic phase was dried by magnesium sulfate and the solvent evaporated under reduced pressure. The residue was purified by column chromatography on silica gel (hexane/ethyl acetate, 6:1) to gives pa-OH as a light-yellow liquid which solidified to a pale-yellow powder upon drying (87.5%).

2.3. Syntheses of pa-OH terminated PCL (pa-PCL)

Hydroxyl groups [24–26] act as initiators for the polymerization of ε-CL polymerization in presence of $Sn(Oct)_2$ [27,28]. In the case of controlled/living polymerization, the molecular weight of pa-PCL can be predicted from the ε-CL/pa-OH molar ratio, as indicated in Table 1. The ring opening polymerization was performed at 120 °C over 24 h as shown in Scheme 1. Various quantities of ε-CL to pa-OH were added under nitrogen into a two-necked flask, equipped with a dry stirring bar, and mixed for 10 min. The flask was placed into an oil bath maintained at 120 °C and the contents were stirred vigorously for ca. 5 min. A certain amount of $Sn(Oct)_2$ in dry toluene was added to the mixture. The crude sample was cooled after 24 h and then dissolved in THF; the solution was poured dropwise into an excess of hexane. The purified polymer was dried in a vacuum oven until constant weight; the yield was determined gravimetrically.

2.4. Reactants preparations

Mixtures of pa-PCL(25 wt%) and B-a type benzoxazine (75 wt%) having several different molecular weights (Table 2) were prepared by solution blending. The mixture was dissolved by stirring in THF; the solution was left to evaporate slowly at 50 °C for 1 day and then cured at 180 °C for 4 h under vacuum to ensure total curing of the co-polybenzoxazine (co-PBZZ). After curing, we obtained a smooth, stiff, hazel-to-brown film. The cured sample was stirred and heated reflux in 0.3 N aqueous $NaHCO_3$ at 90 °C for 24 h to remove the ester group of the labile constituent (PCL). The porous structures were obtained after drying under vacuum in an oven.

2.5. Nuclear magnetic resonance (NMR)

^1H NMR spectra were recorded on a Varian Unity Inova 500 FT-NMR Spectrometer operating at 500 MHz; chemical shifts are reported in parts per million (ppm). Deuterated chloroform was used as the solvent.

2.6. Fourier transform infrared spectroscopy (FT-IR)

FT-IR spectroscopic measurements were conducted on a Nicolet Avatar 320 FT-IR spectrophotometer; 32 scans were collected with a spectral resolution of 1 cm^{-1}. Infrared spectra of the co-polymers were obtained using the conventional NaCl method. The film used in this study was thin enough to obey the Beer–Lambert law. To maintain a dry film, the sample chamber was purged with nitrogen during the measurement process.

2.7. Differential scanning calorimetry (DSC)

The calorimetric measurement was performed using a TA Instruments differential scanning calorimeter (DSC-2010) and conducted under a nitrogen flow of 25 mL/min. The sample was preheated at a scan rate of 20 °C/min from 30 to 240 °C and then maintained at 240 °C for 2 min. The measurement was made using 5–10 mg of sample in a DSC sample cell by cooling to −120 °C quickly from the melt of the first scan. The second scan was conducted at a rate of 20 °C/min from −120 to 250 °C and the value of T_g was taken as the midpoint of the heat capacity transition between the upper and lower points of deviation from the extrapolated liquids and glass lines. Furthermore, we also obtained the values of T_m and ΔH_m.

2.8. Thermogravimetric analyses (TGA)

The thermal stability of the cured sample was investigated using a TA Instruments Q50 apparatus. The cured sample (10–20) mg was placed in a Pt cell and heated from 30 to 800 °C under a nitrogen flow of 60 mL/min at a heating rate of 20 °C/min.

Table 1
Results of the homopolymerization of ε-caprolactone (CL) with various amounts of pa-OH in the bulk at 120 °C and $[CL]/[Sn(Oct)_2] = 1000$; polymerization time: 24 h

Entry	$[M]/[I]$	$M_{n,GPC}$	$M_{n,NMR}$	M_w/M_n	Yield (%)
1a	30	3000	5100	1.15	95.5
1b	120	14,800	28,700	1.54	94.4
1c	200	24,000	41,600	1.71	90.5

Table 2
Curve fitting of fraction of hydrogen-bonding results of the pa-PCL/PBZZ co-polymers at room temperature

Pa-PCL/PBZZ	Free C=O		H-bonded C=O		f_b (%)
	ν (cm^{-1})	A_f (%)	ν (cm^{-1})	A_b (%)	
pa-PCL(M_n=3000), **2a**	1733.5	32.71	1708.4	67.29	57.83
pa-PCL(M_n=14,800), **2b**	1732.2	67.36	1705.7	32.64	24.42
pa-PCL(M_n=24,000), **2c**	1731.5	73.51	1704.8	26.49	19.37

f_b=fraction of hydrogen bonding.

2.9. Field emission scanning electron microscopy (FE-SEM)

The samples of the porous pa-PCL/PBZZ co-polymers were fractured using liquid nitrogen and their cross-sectional morphologies were observed by low-voltage FE-SEM. SEM images were recorded at high magnifications under high vacuum using a TOSHIBA S4700I field emission microscope working at 5 kV with a beam current of 1×10^{-10} A. To increase the resolution of the FE-SEM image, a thin layer of Pt was spun onto the surface of the sample to increase its conductivity; the thickness of this Pt layer was controlled to ca. 10 nm to avoid affecting the actual images.

2.10. Dielectric analyses

Dielectric relaxation data were obtained using a TA Instruments DEA-2970 apparatus, which incorporated a parallel plate cell arrangement and a computer-controlled furnace to ensure that good electrical contact was made between the electrodes and the sample. A flat film is required to increase the accuracy of the measurement of the dielectric constant and, thus, we used the automatic scraper to form such a flat film. The experiment was conducted under a nitrogen flow of 90 mL/min and the thickness of sample was controlled to between 0.125 and 0.75 mm. The dielectric constant and dielectric loss were determined between 0 and 50 °C using a heating rate of 2 °C/min with scan frequencies ranging from 1 to 10^5 Hz.

3. Results and discussion

3.1. Nuclear magnetic resonance analyses

After the cyclization of the oxazine, we observed the characteristic benzoxazine peaks (Ar–CH_2–N and N–CH_2–O units) using ^{1}H NMR spectroscopy. The ^{1}H NMR spectrum ($CDCl_3$, 500 MHz) of pa-OH: δ (ppm) 4.54 (s, 2H, Ar–CH_2–N), 4.60 (s, 2H, Ar–CH_2–OH), 5.38 (s, 2H, N–CH_2–O), 6.76–7.26 (8H, Ar). Furthermore, The ^{1}H NMR spectrum ($CDCl_3$, 500 MHz) of pa-PCL(M_n=24,000, **1c**): δ (ppm) 1.35 (m, 2H, –CH_2–, poly), 1.62 (m, 2H, –CH_2–, poly), 1.62 (m, 2H, –CH_2–, poly), 2.28 (t, 2H, –O(O)CCH_2–, poly), 3.66 (q, 2H, –CH_2OH–, ω-end), 4.03 [t, 2H, –CH_2OC(O)–, poly]. We observed similar results for the other pa-PCL compounds (M_n=3000, **1a**; M_n=14,800, **1b**). Therefore, based on these ^{1}H NMR spectra, we confirmed the successful synthesis of pa-OH and pa-PCL derivatives of various molecular weights.

3.2. Fourier transfer infrared spectroscopy analyses

Fig. 1(a)–(f) display the carbonyl stretching region (1680–1780 cm^{-1}) of the IR spectra, measured at room temperature, of pa-PCL and the pa-PCL/PBZZ co-polymers. The carbonyl stretching for pure pa-PCL is split into two bands at 1734 and 1724 cm^{-1}, as indicated in Fig. 1(a)–(c), which correspond to absorptions by the amorphous and crystalline conformations, respectively. The crystalline conformation at 1724 cm^{-1} of pa-PCL was destroyed

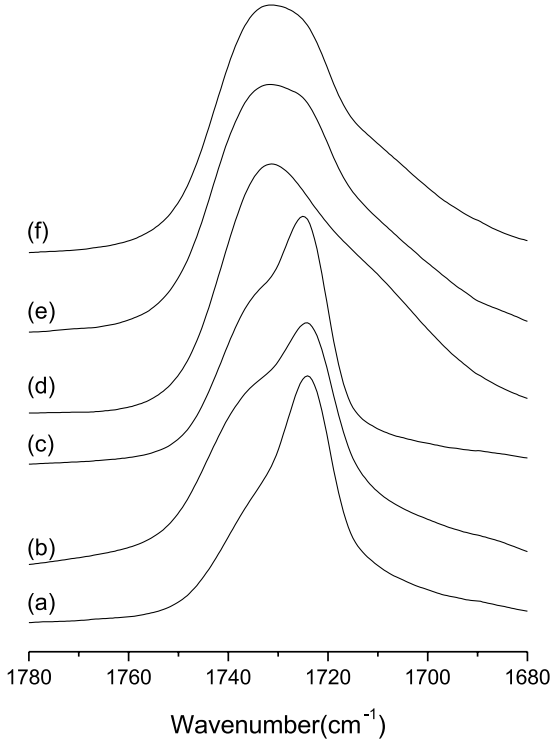

Fig. 1. FT-IR spectra of (a) pa-PCL(M_n=3000, **1a**), (b) pa-PCL(M_n=14,800, **1b**), (c) pa-PCL(M_n=24,000, **1c**), (d) pa-PCL/PBZZ (M_n=3000, **2a**), (e) pa-PCL/PBZZ (M_n=14,800, **2b**), (f) pa-PCL/PBZZ (M_n=24,000, **2c**) recorded at room temperature between 1680 and 1780 cm^{-1}.

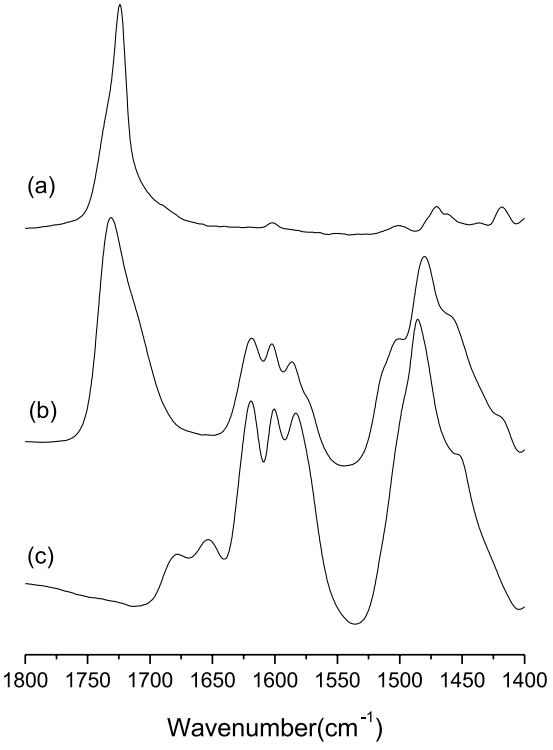

Fig. 2. FT-IR spectra of (a) pa-PCL(M_n=3000, **1a**), (b) pa-PCL/PBZZ (M_n=3000, **2a**), (c) porous PBZZ (M_n=3000, **3a**) recorded at room temperature between 1400 and 1800 cm^{-1}.

substantially after incorporating pa-PCL into the PBZZ backbone as shown in Fig. 1(d)–(f). A small amount of the crystalline conformation at 1724 cm^{-1} of pa-PCL is still present, however, which indicates that pa-PCL and PBZZ are not fully miscible. We assign another band, which appears at ca. 1705 cm^{-1} to the pa-PCL carbonyl groups that are hydrogen bonded to the PBZZ hydroxyl groups. The carbonyl stretching frequency splits into only two major bands at 1732 and 1705 cm^{-1}, which correspond to the free and hydrogen-bonded carbonyl groups, that fit well to the Gaussian function. We calculated the fraction of hydrogen-bonded carbonyl groups using the following equation [29]:

$$f_b^{C=O} = \frac{A_b/1.5}{A_b/1.5 + A_f} \quad (1)$$

where A_f and A_b are the peak areas corresponding to the free and hydrogen-bonded carbonyl groups, respectively. The conversion co-efficient 1.5 is the ratio of these two bands, the free and hydrogen-bonded carbonyl groups. Table 2 summarizes the results from curve fitting. The fraction of the hydrogen-bonded carbonyl groups decreases upon increasing the relative molecular weight of the pa-PCL. In other words, a lower-molecular-weight pa-PCL has better miscibility with PBZZ.

In addition, Fig. 2(a)–(c) present the region from 1400 to 1800 cm^{-1} in the IR spectra, measured at room temperature, of pa-PCL(M_n=3000, **1a**), pa-PCL(M_n=3000)/PBZZ co-polymer (**2a**), and porous PBZZ (**3a**), respectively. It is clear that the carbonyl groups of pa-PCL disappear after the hydrolysis of the pa-PCL/PBZZ co-polymer using $NaHCO_3$. Meanwhile, the characteristic peaks of PBZZ are still present in Fig. 2(c). In other words, a porous PBZZ structure had formed and we confirmed its components by obtaining these FT-IR spectra.

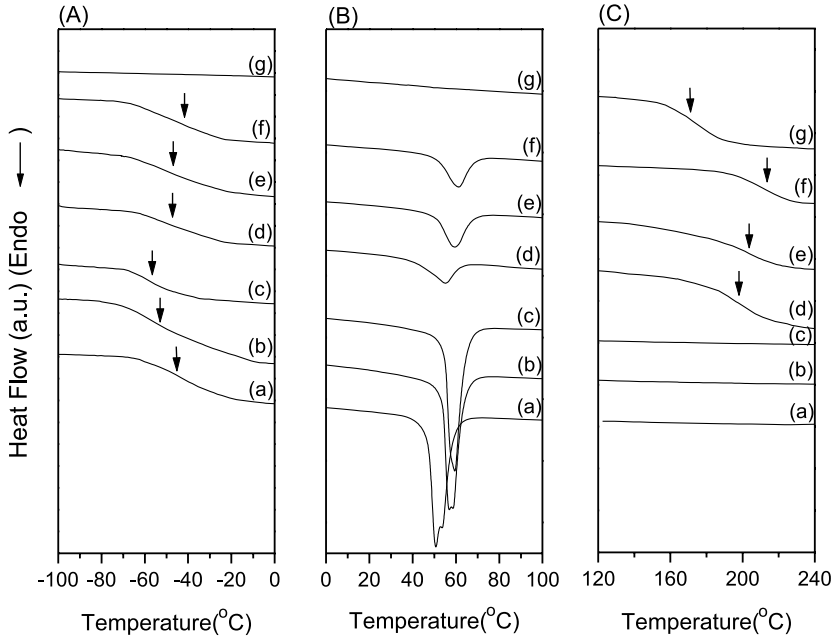

Fig. 3. DSC scans in the ranges from (A) −120 to 0 °C, (B) 0–100 °C, and (C) 120–240 °C of (a) pa-PCL(M_n=3000, **1a**), (b) pa-PCL(M_n=14,800, **1b**), (c) pa-PCL(M_n=24,000, **1c**), (d) pa-PCL/PBZZ (M_n=3000, **2a**), (e) pa-PCL/PBZZ (M_n=14,800, **2b**), (f) pa-PCL/PBZZ (M_n=24,000, **2c**), (g) pure PBZZ.

Table 3
Glass transition temperatures, melting temperatures, and heats of melting of different pa-PCL/PBZZ composites

Component	T_g (°C)	T_m (°C)	ΔH_m (J/g)
Pa-PCL(M_n=3000), **1a**	−45	51	85.2
Pa-PCL(M_n=14,800), **1b**	−54	57	81.4
Pa-PCL(M_n=24,000), **1c**	−58	59	80.9
Pa-PCL(M_n=3000)/PBZZ, **2a**	−47, 198	55	16.5
Pa-PCL(M_n=14,800)/PBZZ, **2b**	−47, 203	59	17.3
Pa-PCL(M_n=24,000)/PBZZ, **2c**	−41, 212	61	18.0
PBZZ	171	–	–

3.3. Differential scanning calorimetry analyses

Fig. 3(A)–(C) and Table 3 display the values of T_g, T_m, and ΔH_m of the various pa-PCL, pa-PCL/PBZZ, and pure PBZZ systems. The pa-PCL/PBZZ co-polymers (**2a**, **2b**, and **2c**) possess two glass transition temperatures, representing pa-PCL and PBZZ, respectively, which is a phenomenon that indicates that pa-PCL and PBZZ are not totally miscible in the amorphous region. Meanwhile, the value of T_m of pa-PCL shifts to higher temperature gradually as it becomes incorporated into the PBZZ matrix, presumably because the cross-linking structure of PBZZ hinders the transfer of heat to the crystalline region of pa-PCL. The crystalline pa-PCL was destroyed substantially, however, upon the DSC measurement as shown in Fig. 3(B) and Table 3; these results are consistent with those obtained from the FT-IR spectra. The DSC results show that these co-polymers were microphase separated, which is a prerequisite for forming porous low-dielectric-constant materials.

3.4. Thermogravimertric analyses

Fig. 4 displays TGA thermograms of (a) pa-PCL, (b) pa-PCL/PBZZ, and (c) pa-PCL/PBZZ after hydrolysis, as a function of the various molecular weights of pa-PCL; Table 4 summarizes the results, including the 5 wt% loss temperatures and char yields. As can be seen, increasing the molecular weight of pa-PCL increase the decomposition temperature in Fig. 4(a). Furthermore, the opposite result of char yield was observed because of the higher or lower

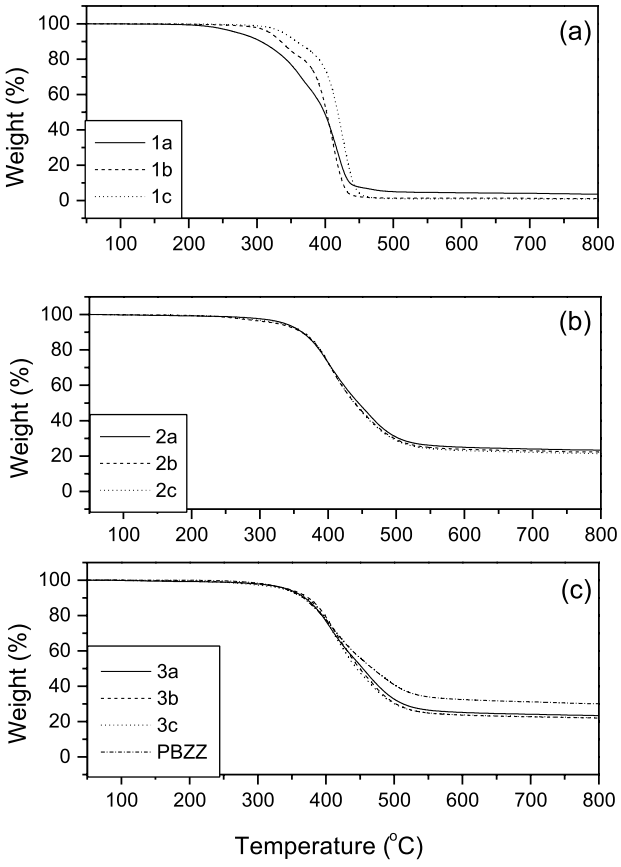

Fig. 4. TGA thermograms of (a) pa-PCL, (b) pa-PCL/PBZZ, and (c) pa-PCL/PBZZ after hydrolysis, as a function of the molecular weight of pa-PCL.

content of the terminal end group of the pa benzoxazine. The 5 wt% loss temperatures of the various pa-PCL/PBZZ mixtures are close as shown in Fig. 4(b), but the tendency of the char yield is similar to that observed for pa-PCL for the same reason suggested for Fig. 4(a). Moreover, after the hydrolysis process, which removes the PCL segment of pa-PCL, the decomposition temperatures increased and are close to that of PBZZ as shown in Fig. 4(c) and Table 4. In other words, these results indicate that the PCL domains were completely removed from the pa-PCL/PBZZ co-polymers after hydrolysis.

Table 4
The 5 wt% weight-loss temperatures of different pa-PCL composites recorded under a N_2 environment

Component	5 wt% Weight loss (°C)	Char yield (%) at 800 °C
pa-PCL(M_n=3000), **1a**	270	3.6
pa-PCL(M_n=14,800), **1b**	326	1.2
pa-PCL(M_n=24,000), **1c**	334	0.9
pa-PCL(M_n=3000)/PBZZ, **2a**	328	23.3
pa-PCL(M_n=14,800)/PBZZ, **2b**	329	22.2
pa-PCL(M_n=24,000)/PBZZ, **2c**	330	21.4
pa-PCL(M_n=3000)/PBZZ after hydrolysis, **3a**	343	23.4
pa-PCL(M_n=14,800)/PBZZ after hydrolysis, **3b**	343	22.0
pa-PCL(M_n=24,000)/PBZZ after hydrolysis, **3c**	337	22.1
PBZZ	340	30.1

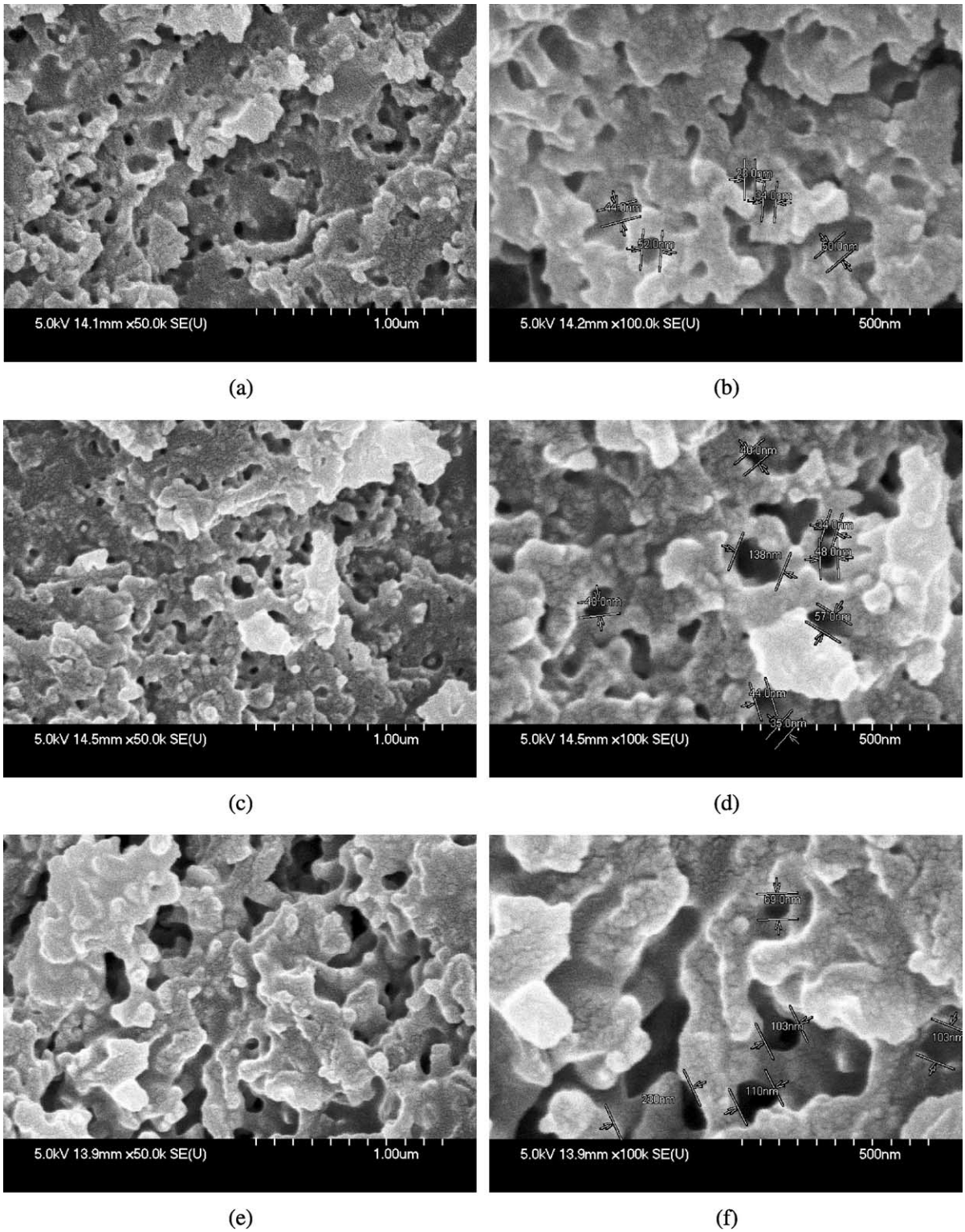

Fig. 5. FE-SEM images of cross-sections of pa-PCL/PBZZ after hydrolysis recorded at high magnifications: (a) (**3a**, 50KX), (b) (**3a**, 100KX), (c) (**3b**, 50KX), (d) (**3b**, 100KX), (e) (**3c**, 50KX), (f) (**3c**, 100KX).

3.5. Scanning electron microscopy analysis

We also investigated the pore morphologies of the pa-PCL/PBZZ co-polymers by FE-SEM after removal of the pa-PCL segment. Fig. 5(a)–(f) present SEM micrographs of fracture surfaces (cross-sections) of the pa-PCL/PBZZ co-polymers, which were frozen in liquid nitrogen after hydrolysis of the PCL segments using $NaHCO_3$. Each of

these systems possesses a pa-PCL content of 25 wt%, but notable variations in morphology occur as a result of their different molecular weights. We observe heterogeneous morphologies in Fig. 5(a)–(f), i.e. the co-polymers were micro-phase separated after the pa-PCL segment was incorporated into the PBZZ matrix. For the pa-PCL(M_n = 3000)/PBZZ system in Fig. 5(a) and (b), it can be seen that the pores are dispersed uniformly in the continuous matrix, and these pores have diameters that are <50 nm. Furthermore, we attribute these voids to the pa-PCL rich phase, whereas the continuous phase is the PBZZ matrix. Upon increasing the molecular weight of pa-PCL from $M_n = 3000$ to 14,800 and 24,000, the porous structures display remarkably different morphologies as shown in Fig. 5(c)–(f). These morphologies incorporate pore sizes that vary in the range from tens to hundreds of nanometer as these voids began to aggregate, interconnect, and exhibit irregular shapes. Meanwhile, the pore size distribution became broader on the cross-sectional surface. The pore size and distribution of **3a**, **3b** and **3c** are 41.6 ± 10.3, 54.5 ± 34.0 and 61.9 ± 27.7 nm, respectively. The results of these morphological studies reveals that the pa-PCL having $M_n = 3000$ is the one most suitable for forming the most evenly distributed porous minor phase within the PBZZ matrix. Most importantly, it also gives the lowest degree of pore interconnection; a closed or isolated pore structure is usually preferred to an open or connected pore structure because connected pores may create current path leakage and result in solvent absorption during wet cleaning processes, which allows damaging gases to penetrate deep into the film during the etching and dry resist stripping processes.

3.6. Dielectric analysis

Because the dielectric constants of gases are not much different from that of a vacuum ($k = 1$), the incorporation of free space or pores is an attractive method for decreasing the dielectric constants of films, even though porous and low-density materials pose greater challenges in both characterization and integration. The key to determining a material's properties depends directly on integration issues, including porosity, pore size, and size distribution, and the extent of interconnection. Increasing the porosity decreases the dielectric constant, but it tends to reduce the material's mechanical properties. In general, the maximum porosity is controlled to between 25 and 30%. The average pore size must be substantially smaller, and the size distribution (uniform or random) may affect the mechanical properties of the film. Therefore, it is necessary to control the frequency of large pores, which would constitute void defects between metal lines. Furthermore, the pa-PCL(M_n = 3000)/PBZZ (**3a**) system possesses a relative closed and well-distributed pore structure, as evidenced from the FE-SEM images, which implies that it is most suitable for applications as a low-dielectric-constant material.

The PBZZ porous structure was created after removing the PCL segment from the pa-PCL/PBZZ co-polymer; the value of its dielectric constant is lower than that of virgin PBZZ. In Fig. 6(a), we observe that the dielectric constant of the PBZZ decreases from 3.56 to 1.95 upon varying the pa-PCL molecular weight at a constant pa-PCL loading (25 wt%). Based on the DEA measurement, pa-PCL(M_n = 3000)/PBZZ (**3a**) gives the lowest value of k. Fig. 6(b) displays the dielectric constant of different pa-PCL(M_n = 3000) loading in the PBZZ matrix. As would be expected, the decrease in the value of k from 3.56 to 1.95 occurred as the pa-PCL content was increased from 0 to 25 wt% after hydrolysis.

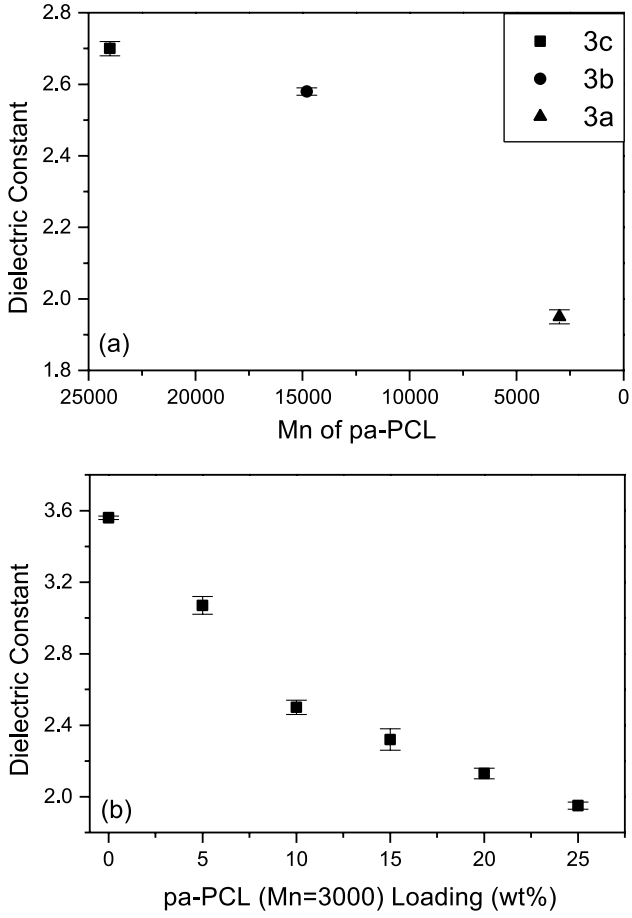

Fig. 6. Dielectric constants of PBZZ materials obtained using (a) pa-PCL of different molecular weights at a constant loading of 25 wt% at 10^5 Hz and 298 K and (b) different loading percentages of the pa-PCL(M_n = 3000).

4. Conclusions

We have developed a new class of nanoporous PBZZ material that has a substantially lower dielectric constant by using the pa-PCL as the labile constituent. FE-SEM images show that the labile polymer micro-phase separates in the PBZZ matrix with domain sizes that depend upon the molecular weight of pa-PCL used. These pores were generated when the pa-PCL was eliminated by hydrolysis

of the pa-PCL/PBZZ co-polymer. A transition from isolated to interconnected pores was observed when the molecular weights of pa-PCL were increased from $M_n = 3000$ to 24,000. These porous materials have dielectric constants, relative to that of the virgin PBZZ (3.56), that are as low as 1.95 at 10^5 Hz and 298 K.

References

[1] Ho PS, Leu J, Lee WW. Low dielectric constant materials for IC application. New York: Springer; 2002.
[2] Maier G. Prog Polym Sci 2001;26:3.
[3] Nalwa HS, editor. Handbook of advanced electronic and photonic materials and devices, vol. 4. San Diego, CA: Academic Press; 2001.
[4] Treichel H, Ruhl G, Ansmann P, Wurl R, Muller CH, Dietlmeier M. Microelectron Eng 1998;40:1.
[5] Yang P, Zhao D, Chmelka BF, Stucky GD. Chem Mater 1998;10: 2033.
[6] Charlier Y, Hedrick JL, Russell TP, Jonas A, Volksen W. Polymer 1995;36:987.
[7] Hedrick JL, Carter KR, Cha HJ, Hawker CJ, DiPietro RA, Labadie JW, et al. React Funct Polym 1996;30:43.
[8] Kim HC, Volksen W, Miller RD. Chem Mater 2003;15:609.
[9] Nguyen CV, Carter KR, Hawker CJ, Hedrick JL, Jaffe RL, Miller RD, et al. Chem Mater 1999;11:3080.
[10] Carter KR, Dipietro RA, Sanchez MI, Russell TP. Chem Mater 1997; 9:105.
[11] Carter KR, Dipietro RA, Sanchez MI, Swanson SA. Chem Mater 2001;13:213.
[12] Yang S, Mirau PA, Pai CS, Nalamasu O, Reichmanis E, Lin EK, et al. Chem Mater 2001;13:2762.
[13] Yang S, Mirau PA, Pai CS, Nalamasu O, Reichmanis E, Pai JC, et al. Chem Mater 2002;4:69.
[14] Hung QR, Volksen W, Huang E, Toney M, Frank CW, Miller RD. Chem Mater 2002;14:3676.
[15] Hung QR, Kim HC, Huang E, Mecerreyes D, Hedrick JL, Volksen W, et al. Macromolecules 2003;36:7661.
[16] Kim HC, Wilds JB, Hinsberg WD, Johnson LR, Volksen W, Magbitang T, et al. Chem Mater 2002;14:4628.
[17] Hedrick JL, Russell TP, Labadie J, Lucas M, Swanson S. Polymer 1995;36:2685.
[18] Lezcano EG, Coll CS, Prolongo MG. Polymer 1996;37:3603.
[19] de Juana R, Cortazar M. Macromolecules 1993;26:1170.
[20] Kuo SW, Chang FC. Macromolecules 2001;34:7737.
[21] Ishida H, Sanders DP. Macromolecules 2000;33:8149.
[22] Wang YX, Ishida H. Macromolecules 2000;33:2839.
[23] Su YC, Chang FC. Polymer 2003;44:7989.
[24] Ning X, Ishida H. J Polym Sci Part B: Polym Phys 1994;32:921.
[25] Ydens I, Rutot D, Degee P, Six JL, Dellacherie E, Dubois P. Macromolecules 2000;33:6713.
[26] Jeon O, Lee SH, Kim SH, Lee YM, Kim YH. Macromolecules 2003; 36:5585.
[27] Nederberg F, Bowden T, Hilborn J. Macromolecules 2004;37:954.
[28] Shuai X, Merdan T, Unger F, Wittmar M, Kissel T. Macromolecules 2003;36:5751.
[29] Coleman MM, Graf JF, Painter PC. Specific interactions and the miscibility of polymer blends. Lancaster, PA: Technomic; 1991.